The Structure and Mechanical Properties of Metallic Nanocrystals

C. SURYANARAYANA and F.H. FROES

Metallic nanocrystals are ultrafine-grained polycrystalline solids with grain sizes in the range of 1 to 10 nm in at least one dimension. Because of the extremely small dimensions, a large fraction of the atoms in these materials is located at the grain boundaries, and thus, they possess novel, and often improved, properties over those of conventional polycrystalline or glassy materials. In comparison to more conventional materials, nanocrystalline materials show a reduced density; increased thermal expansion, specific heat, and strength; a supermodulus effect; and extremely high diffusion rates. Traditionally brittle materials can be made ductile by nanostructure processing. At present, there is considerabe confusion on the nature of the microstructure and mechanical properties of the nanocrystalline materials, especially of the equiaxed (three-dimensional, 3-D) type. The present article reviews the current understanding of nanocrystals and evaluates the data available on structure and mechanical properties of nanocrystalline metals.

I. INTRODUCTION

NANOCRYSTALLINE materials (also referred to as nanostructures, nanophase materials, or nanometer-sized crystalline solids) are single-phase or multi-phase polycrystals, the crystal size of which is of the order of a few (typically 1 to 10) nanometers (1 nm = 10^{-9} meter) in at least one dimension.[1–7] Thus, they can be basically equiaxed in nature[1,5,7] and will be termed nanostructure crystallites [three-dimensional (3-D) nanostructures], or they can consist of a lamellar structure,[8] and will be termed a layered nanostructure [one-dimensional (1-D) nanostructure], or they can be filamentary in nature[9] [two-dimensional (2-D) nanostructure]. Table I shows this classification and Figure 1 illustrates the three types of nanostructures schematically. The magnitudes of length and width are much greater than thickness in the layered nanocrystals, and length is substantially larger than width in filamentary nanocrystals. The nanocrystalline materials may contain crystalline, quasicrystalline, or amorphous phases and can be metals, ceramics, or composites. It has been shown that these materials have properties often superior to those of the conventional coarse-grained polycrystalline materials.[1,5,7]

A great deal of effort has gone into the synthesis and characterization of these novel materials, with emphasis on the nanostructure crystallites and, to a lesser extent, on the layered structures. Relatively few investigations have been reported on the filamentary nanocrystals. Recently, greater attention is being paid to the development of nanocrystalline ceramics, since it has been demonstrated that they can be sintered at relatively low temperatures[10] and can also exhibit improved ductility,[11] and even potential superplasticity,[12] in the nanocrystalline state. A number of research groups are currently devoting their efforts to understanding of the nature and properties of the nanocrystalline materials and exploiting them for industrial applications.[1–7] Although useful properties (*e.g.*, lowered sintering temperature and improved fabricability) have been reported for ceramic materials with nanometer-sized grains, the present review will restrict itself to a discussion of the nanocrystalline metals. More specifically, structure and mechanical properties will be considered in detail, with emphasis on rationalizing conflicting reports in this area.

II. CHARACTERISTICS

A schematic representation of a hard-sphere model of an equiaxed nanocrystalline metal is shown in Figure 2. Two types of atoms can be distinguished: crystal atoms with nearest-neighbor configurations corresponding to the lattice and boundary atoms with a variety of interatomic spacings, differing from boundary to boundary. A nanocrystalline metal contains typically a high number of interfaces ($\sim 6 \times 10^{25}$ m^{-3}) with random orientation relationships, and consequently, a substantial fraction of atoms lies in the interfaces. Assuming that grains have the shape of spheres or cubes, the volume fraction of nanocrystalline materials associated with the boundaries was calculated[13] as

$$C_t = 3\Delta/d$$

where Δ is the average grain boundary thickness and d is the average grain diameter. Thus, these volume fractions can be as much as 50 pct for 5-nm grains and decrease to about 30 pct for 10-nm grains and 3 pct for 100-nm grains. Hence, nanocrystalline metals can be considered to consist of two structural components — crystallites with long-range order and disordered interfacial component. If the local atomic environments of

C. SURYANARAYANA and F.H. FROES, Professor and Director, respectively, are with the Institute for Materials and Advanced Processes, University of Idaho, Moscow, ID 83843-4195.

This invited overview is based on a presentation made in the symposium "Structure and Properties of Fine and Ultrafine Particles, Surfaces and Interfaces" presesnted as part of the 1989 Fall Meeting of TMS, October 1–5, 1989, in Indianapolis, IN, under the auspices of the Structures Committee of ASM/MSD.

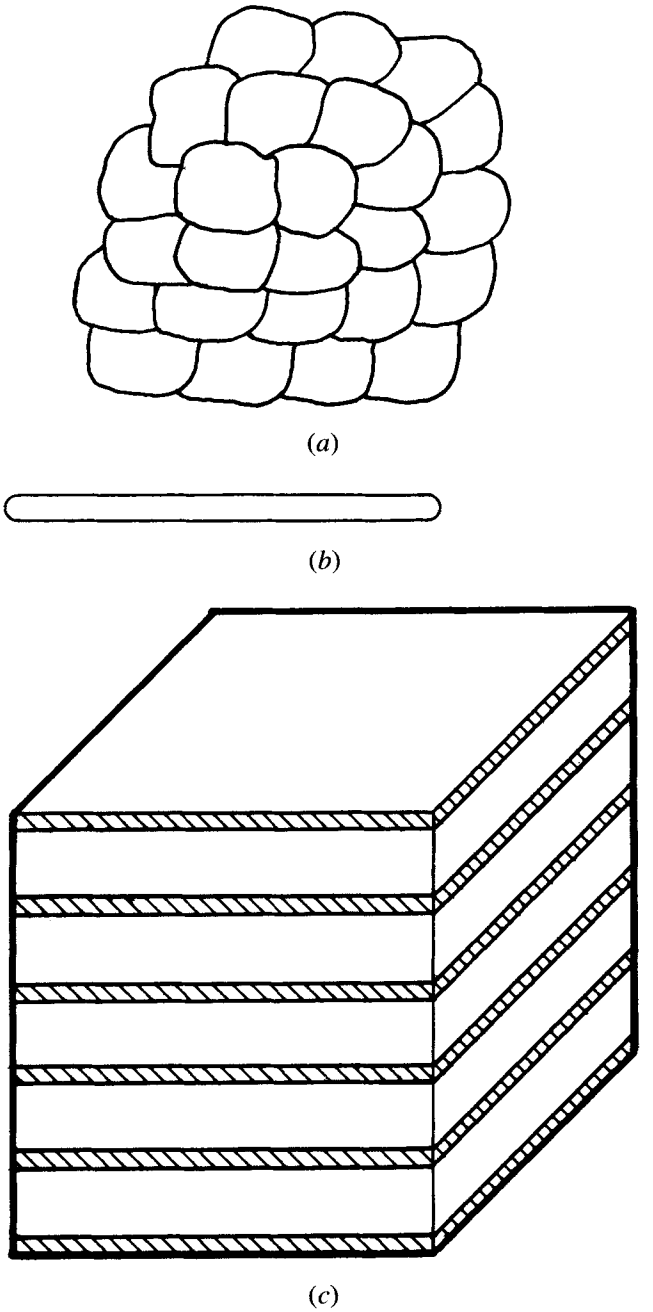

Fig. 1 — Schematic representation of (*a*) equiaxed, (*b*) filamentary, and (*c*) lamellar nanocrystals. The equiaxed nanocrystals have nanometer dimensions in all three directions, while they are only nanodimensional for the thickness and width of the filamentary and thickness of the lamellar nanocrystals, respectively.

the interfacial atoms are averaged, there would be neither long-range nor short-range order. This structure is thus in contrast to that obtained both in crystalline and amorphous materials.

The grain boundaries in the nanocrystalline metals are relatively unrelaxed, a state somewhat similar to rapidly quenched metallic glasses[14] in that the system of boundary atoms has a local but not global energy minimum; thus, the material is in a metastable condition.

Because of the fineness of the grain structure, stability is often a concern; however, the layered nanostructure,

Table I. Classification of Nanocrystalline Materials

Dimensionality	Designation	Typical Method of Synthesis
Three-dimensional	crystallites (equiaxed)	gas condensation mechanical alloying
Two-dimensional	filamentary	chemical vapor deposition
One-dimensional	layered (lamellar)	vapor deposition electrodeposition

in particular, can be quite stable. Significant grain growth (doubling of the crystal size in 24 hours) was observed in single-phase nanostructure crystallites at ambient temperature or below only when the equilibrium melting temperature T_m was lower than about 600 °C. Grain growth was retarded for higher T_m metals, *e.g.*, for Cu up to ~100 °C, for Pd up to ~250 °C,[4] and for Ti-Mg up to ~450 °C.[15] The nature of the chemical bond was also found to significantly affect the grain growth. Just as in conventional polycrystals, grain growth in nanocrystalline materials may be inhibited by second-phase particles[16] and/or impurity drag. The stability of the multiphase nanocrystals depends on the mutual solubility of the phases involved; the lower the solubility, the lower the grain growth.

III. SYNTHESIS

In principle, any method capable of producing very fine grain-sized polycrystaline materials can be utilized to produce nanocrystalline metals. However, nanostructure crystallites have generally been prepared by modified gas-condensation methods,[17,18] while the layered nanostructures are synthesized either by vapor deposition[8] or by electrodeposition.[19] Other potential methods for preparing these materials include mechanical alloying (MA),[20] molecular beam epitaxy,[21] rapid solidification from the liquid state,[22,23] ion beam,[2] reactive sputtering,[2] sol-gel,[2] and chemical vapor

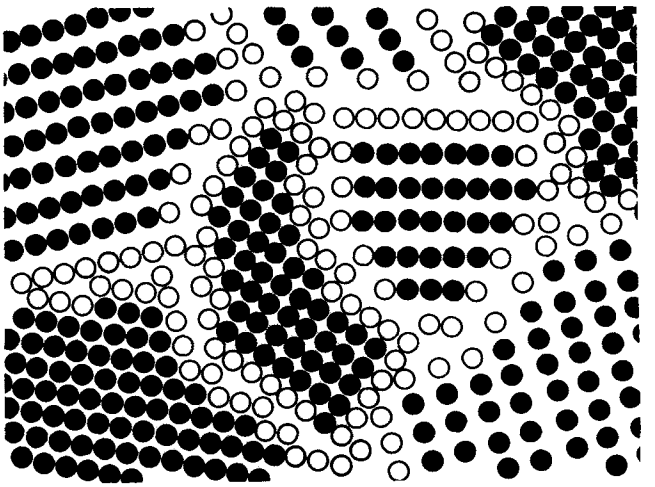

Fig. 2 — Schematic representation of an equiaxed nanocrystalline metal distinguishing between the atoms associated with the individual crystal grains (filled circles) and those constituting the boundary network (open circles).[1]

deposition[24] processes. The grain size, morphology, and texture can be varied by suitably modifying/controlling the process variables in each of these methods.

Controlled crystallization of the amorphous phases produced by any of the above methods (*e.g.*, rapid solidification or electrodeposition) can also be utilized to produce nanocrystalline metals.[23,25,26]

Even though all of the above methods have been used with different levels of success to produce different nanocrystalline materials, only gas condensation, vapor deposition, electrodeposition, and mechanical alloying techniques will be described in view of their widespread use and also the potential of these methods to produce bulk quantities of material.

A. *Gas Condensation Method*

Figure 3 shows a schematic diagram of the gas-condensation method for the production of equiaxed nanocrystals.[3] The system consists essentially of an ultrahigh vacuum (UHV) chamber equipped with a turbomolecular pump, evacuated to about 10^{-7} Pa. The chamber is then back-filled with an inert gas such as He to a pressure of about 1 KPa. The material to be produced in the nanocrystalline state is then evaporated in a refractory metal boat using conventional methods [such as resistive heating (most common), radio-frequency heating, sputtering, electron beam, laser/plasma heating, or ion sputtering]. As a result of interatomic collisions with the helium atoms in the chamber, the evaporated metal atoms lose their kinetic energy and condense in the form of small crystals of loose powder which accumulate, due to convective flow, on a vertical liquid nitrogen-filled cold finger. The crystal size of the powder is typically a few nanometers. Two evaporation sources allow blended mixtures of powders, in which case the cold finger can be rotated to achieve better mixing.

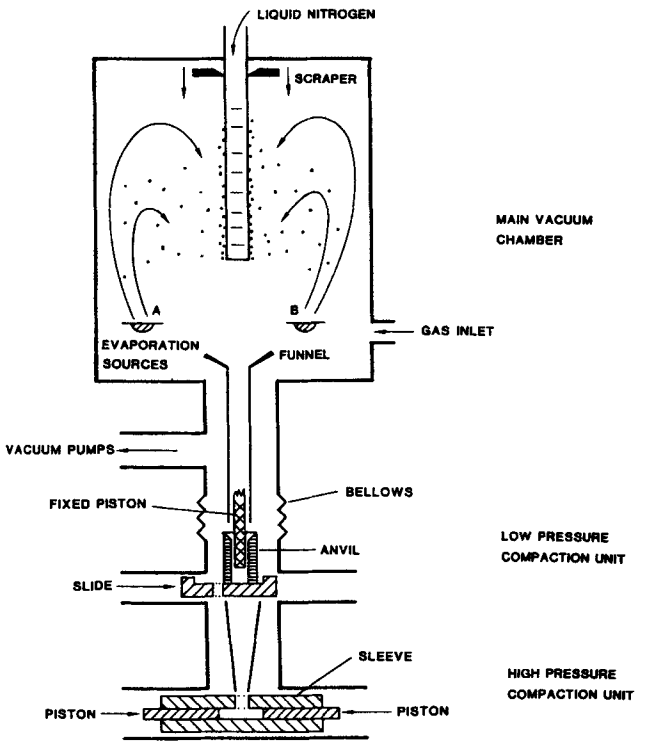

Fig. 3—Schematic representation of a gas-condensation chamber for the synthesis of nanocrystalline materials.[3]

After restoring high vacuum, the powder is stripped off the cold finger by moving an annular TEFLON* ring down the length of the tube into a compaction device. Compaction is carried out in a two-stage piston-and-anvil device initially at low pressures in the upper chamber to produce a loosely compacted pellet, which is then transferred in the vacuum system to a high-pressure unit where final compaction takes place at a pressure of about 5 GPa with tungsten carbide pistons. The scraping and compaction process also is carried out under UHV conditions to maintain cleanliness of the particle surfaces (and subsequent interfaces) and also to minimize the amount of any trapped gases. High densities of as-compacted samples have been measured with values of about 75 to 90 pct of bulk density for metal samples.[1,4]

*TEFLON is a trademark of E.I. Du Pont de Nemours & Company, Inc., Wilmington, DE.

The particle size in this method is dependent upon the inert gas pressure, the evaporation rate, and the gas composition.[17,18] Extremely fine particles can be produced by decreasing either the gas pressure in the chamber or the evaporation rate and by using light (such as He) rather than heavy inert gases (such as Xe). It has been recently shown that control of the inert gas pressure affects not only the particle size but also the resulting phase.[27]

B. *Vapor Deposition*

While versatile, the vacuum deposition techniques are often difficult to control, require expensive equipment, and are not amenable to the fabrication of large structures, particularly those having complex shapes. Control difficulties are inherent in vacuum methods, because the depositing atoms generally arrive at the substrate surface with considerable excess energy so that some disordered growth and interdiffusion are inevitable. However, Bickerdike *et al.*[8] have described a semicommercial scale electron beam vapor deposition process (Figure 4(a)) which results in alternate layers of aluminum (20- to 1600-nm thick) and a second metal (0.1- to 20-nm thick Cr, Fe, Mg, Mn, Ni, or Ti). The vapor was condensed on a temperature-controlled disk-shaped aluminum alloy collector with a polished surface which can be rotated about a vertical axis. Deposits 160 mm in diameter were obtained at rates of 1 to 3 mm/h, thus providing adequate layered nanocrystalline material for mechanical property evaluation.

C. *Electrodeposition*

Electrodeposition of multilayered metals can be achieved using either two separate electrolytes or much more conveniently from one electrolyte by appropriate control of agitation and the electrical conditions (particularly voltage) (Figure 4(b)).[19,28] These processes can be precisely controlled *via* the electrode potential and solution mass transport, require minimal capital investment, and can be applied to the fabrication of parts of

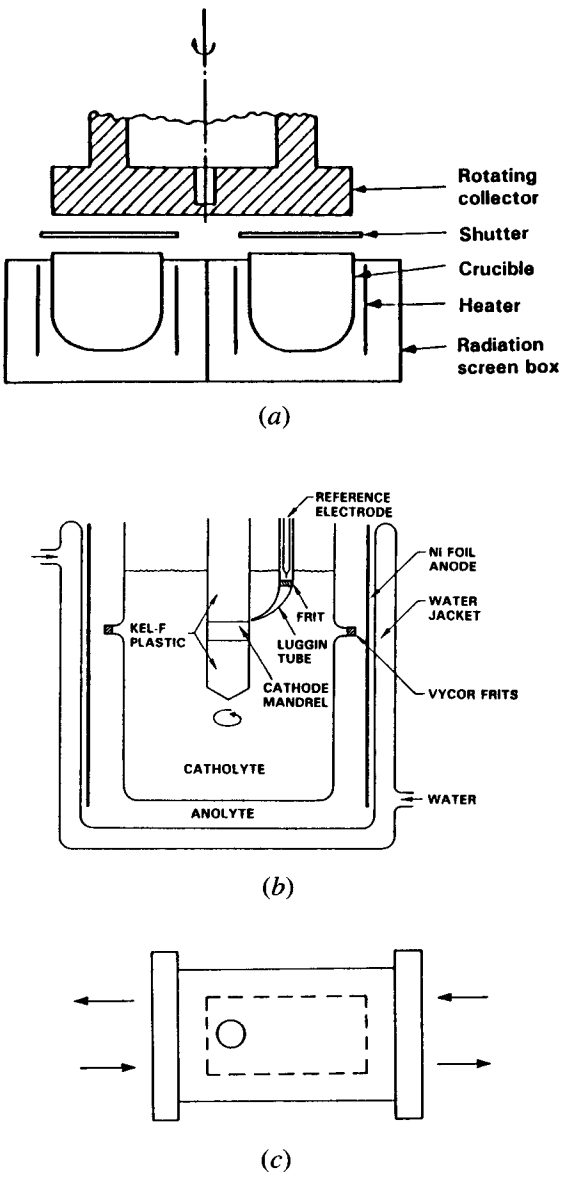

Fig. 4—Schematic cross-sectional representation of (*a*) rotating collector vapor deposition apparatus,[8] (*b*) cell for electrodeposition, and (*c*) MA techniques for synthesizing nanocrystalline specimens.

almost any shape or size. Deposition rates (at the 10-nm layer level) are about 0.05 mm/h, but the process is non-labor intensive and can run automatically for long periods of time. Further, multilayer structures with specific textures can also be easily synthesized using the electrodeposition techniques.[29] Also, 3-D nanostructure crystallites can be prepared using this method by utilizing the interference of one ion with the deposition of the other. The size of the particles can be controlled precisely *via* the concentration of solution species, the deposition voltages/currents, and bath agitation modulations.

Some of the conventional test methods are often not strictly applicable to vacuum-deposited thin films.[30] The slightly thicker deposits obtained in the electrodeposition process are much easier to test and with greater reliability.

Multilayer structures with nanometer-scale thicknesses have also been produced by various other deposition processes, such as sputtering, molecular beam epitaxy, and chemical vapor deposition. Molecular beam epitaxy is an extremely well-controlled deposition technique, and many artificially structured materials with submicron dimensions along the growth direction have been produced; however, this is not a volume production method.

D. *Mechanical Alloying*

Mechanical alloying consists of repeated welding, fracturing, and rewelding of powder particles in a dry high-energy ball charge.[20,31,32] In this process, mixtures of elemental or prealloyed powders are subjected to grinding under a protective atmosphere in equipment capable of high-energy compressive impact forces such as attrition mills, vibrating ball mills, and shaker mills. A majority of the work on nanocrystalline materials has been carried out in highly energetic small shaker mills (*e.g.*, SPEX* model 8000) agitated at a high frequency involving motion in three orthogonal directions; but the amplitude of the motion is greatest in one direction (Figure 4(c)). The intimate mixing of the constituent metals on a very fine scale can result in the formation of several metastable phases. It has been shown recently that materials with nanometer-sized grains can be synthesized by MA of elemental powders,[33–36] intermetallic compound powders,[33,37–41] or immiscible powders.[42–46] The grain size is a function of the energy input into the mill and milling time. However, a few hours of milling is enough in most cases to produce nanometer-sized grains. Control of impurity content, especially in reactive metals, is difficult using the MA technique. However, the production of bulk quantities of powder followed by consolidation makes the MA approach an attractive, commercial-scale processing route.

*SPEX is a trademark of Sytech Corporation, Houston, TX.

IV. STRUCTURE

In order to understand the interrelationship between structure and properties, nanocrystalline materials need to be characterized on both atomic and nanometer scales. The microstructural features of importance include (1) grain size, distribution, and morphology, (2) the nature and morphology of grain boundaries and interphase interfaces, (3) perfection and nature of intragrain defects, (4) composition profiles across grains and interfaces, and (5) identification of residual trapped species from processing. In the case of layered nanostructures, the features of importance are (1) thickness and coherency of interfaces, (2) composition profiles across interfaces, and (3) nature of defects.

There are a vast array of experimental techniques that can yield structural information on nanocrystalline materials. These include "direct" microscopic techniques such as transmission electron microscopy (TEM), scanning tunneling microscopy (STM), field-ion microscopy (FIM), and the less direct electron, X-ray, and neutron diffraction techniques. Indirect spectroscopic tools, such as extended X-ray absorption fine structure, nuclear

magnetic resonance, Raman and Mössbauer spectroscopies, and positron lifetime spectroscopy, have also been used. Other useful tools employed include differential scanning calorimetry, mass spectroscopy, X-ray fluorescence, atomic absorption spectroscopy, Auger electron spectroscopy, and hydrogen absorption.

Owing to the ultrafine scale of these materials, traditional characterization tools such as TEM and X-ray and neutron diffraction are both necessary and useful to understand the structure of nanocrystalline materials. However, for microchemical analysis on the requisite fine scale, further advances in the state-of-the-art of instrumental capabilities will be necessary to obtain the desired lateral scale resolution. Only atom-probe FIM or STM seem to offer the required lateral scale resolution for such chemical mapping at present.

Due to limitations of space, details of the results from all of the above techniques (except TEM) will not be presented here. The interested reader is referred to a recent comprehensive review by Gleiter[1] for details of results from other methods.

The microstructure of nanocrystalline metals has been investigated by high-resolution TEM. These studies indicated that the nanocrystalline metals consist of small crystallites of different crystallographic orientations separated by grain boundaries. Figure 5 shows an electron micrograph of nanometer-sized crystals observed in mechanically alloyed Ti-3 wt. pct Mg alloy,[46] while Figure 6 shows a high-resolution transmission electron micrograph recorded from a nanocrystalline Cu specimen synthesized by the gas-condensation method.[47] From such micrographs (as well as from field-ion micrographs and by small-angle X-ray or neutron scattering data), grain sizes and their distributions can be determined. The grains exhibit typically narrow log-normal size distributions.

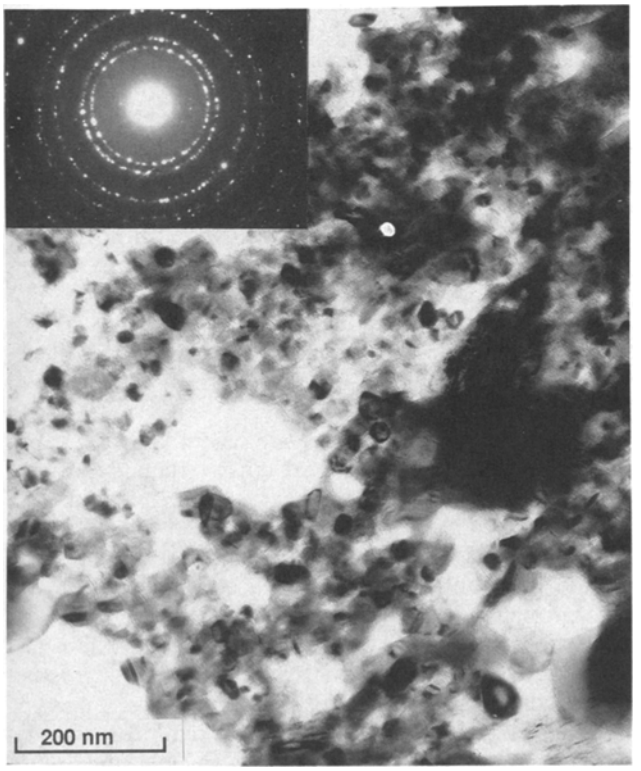

Fig. 5—Electron micrograph showing the size and distribution of nanocrystals in a mechanically alloyed Ti-3 wt pct Mg alloy.[46]

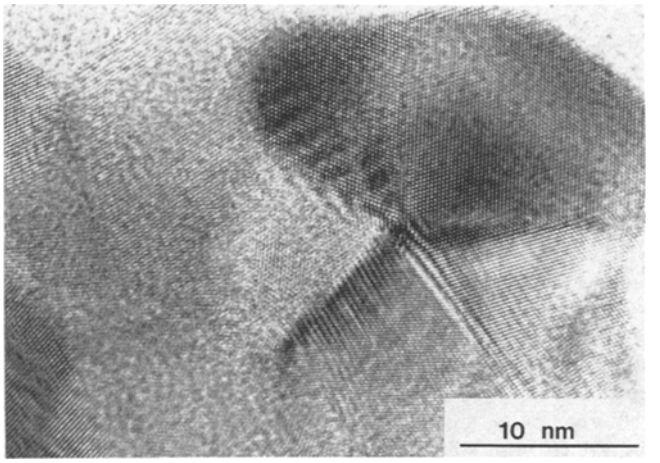

Fig. 6—High-resolution electron micrograph of nanocrystalline copper sample produced by the gas-condensation technique.[47]

The following features may be noted from the high-resolution electron micrographs:

(1) Most of the ultrafine grains exhibit fringe contrast.
(2) The fringes abruptly stop in each grain at the grain boundary, indicating that there is little or no atomic disorder perpendicular to the imaged planes.
(3) The grain boundary planes are basically flat but exhibit some local faceting,[48] probably to bring the planes from both grains into registry.
(4) Neither voids nor dislocations have been observed in these investigations, even though positron annihilation spectroscopy[10,49] and precise densitometry and porosimetry[50,51,52] measurements have clearly indicated the presence of porosity in nanocrystalline metals. Nieman *et al.*[47] report, however, observation of abundant twinning and low-index, faceted crystal regions.

Gleiter and co-workers[1,4] have interpreted most of their results in terms of a two-component microstructure—perfect long-range ordered atomic arrangement in the grains and a random grain boundary component. However, recent results on high-resolution electron microscopy and computer simulation of grain boundaries in nanocrystalline palladium have indicated that the interface atomic structure in nanocrystalline metals is not fundamentally different from that observed in coarser grained polycrystals.[48]

The results of high-resolution TEM have to be interpreted with care. First, electron microscopic characterization of nanocrystalline materials has been done under less than UHV conditions, making the influence of impurities an important consideration. Further, the influence of the high-energy electron beam on the shape and stability of the nanostructures is yet to be defined. Second, since very thin specimens (usually the thickness is less than the crystal diameter) are required for high-resolution TEM, the 3-D crystal arrangement of a bulk nanocrystalline specimen gets transformed into a 2-D arrangement. This process may change the boundary structure as it alters the forces between neighboring crystals

and induces new forces due to the energy of the free surface. Further, due to the high diffusivity in nanocrystalline materials,[1,7] atoms may diffuse from the free surface of a thin specimen into the grain boundaries at ambient temperatures within a time much shorter than the time for specimen preparation, leading to changes in the boundary structure.

From the high-resolution TEM studies, one can, however, conclude that (a) the atoms constituting the boundaries in nanocrystalline materials rearrange themselves into relatively low-energy configurations and (b) the local driving forces for grain growth are relatively small, despite the large amount of energy stored in the many grain boundaries.

Direct evidence for an accurate structure of the grain boundary is difficult to obtain in view of the relaxation at surfaces; results from FIM and STM are required to shed new light on the structure of the boundaries in the nanocrystalline materials.

The nanocrystalline metals pick up a significant amount of impurities both during the evaporation-condensation and compaction stages. While the metallic impurities can range from 10^{-4} to 5 at. pct, the oxygen content was found to vary from 4 at. pct (for high oxygen affinity metals) to 1 at. pct (for low oxygen affinity metals) with no baking in the evaporators; this can be reduced to about 10^{-2} at. pct with baking. There is considerable impurity (both metallic and interstitial) pickup during the MA processing also. This fact has to be taken into account while evaluating the properties of the nanocrystalline materials.

In the layered and filamentary nanostructures, the nature of interfaces is just beginning to be evaluated and not much information is presently available.

V. MECHANICAL PROPERTIES

Nanocrystalline materials can be visualized as comprising two structural components: crystallites with long-range order and the disordered gaslike interfacial component representing the variety of interatomic spacings in the different types of interfaces. This disordered structure, in particular, which is not constrained to thermal equilibrium conditions, offers the prospect of novel physical and mechanical behavior.[53] Novel characteristics include anomalously high diffusivity[54,55,56] and reactivity leading to use in catalytic and adsorption processes, the alloying of conventionally insoluble or low solubility elements because of the more open grain boundary structure,[4,16,46,57] and the ductile behavior of the nanocrystalline ceramics[11,12] and intermetallic compounds.[58] A summary of the equiaxed nanocrystalline material properties compared with those of coarse-grained polycrystals and metallic glasses is given in Table II.

Since the structure of nanocrystalline materials is significantly different from conventional polycrystalline and amorphous materials, the structure-related mechanical properties of nanocrystalline materials are expected to be significantly different.

A. *Equiaxed Nanocrystals*

The elastic constants of nanocrystalline materials have been measured by a variety of methods[59,60] and found to be reduced by 30 pct or less (Table II). These results were interpreted as due to the large free volume of the grain boundary component resulting from the increased average interatomic spacings in the boundary regions.

The most significant change resulting from a reduction in the grain size to the nanometer level is an increase in the strength and hardness, which also is the least understood and most controversial area. While the 0.2 pct yield strength of a 25-nm grain size Cu sample was reported to be 185 MPa, that of a sample with a 50-μm grain size was only 83 MPa[50,51,61] (Figure 7). Similar results have also been reported for nanocrystalline Pd,[50,61,62] Fe,[34] Ni,[63] Nb_3Sn,[41] and TiO_2[64] samples. A reduction in hardness with grain size was, however, reported for Ni-P[25] and by Chokshi *et al.*[65] for Cu and Pd specimens.

The Hall-Petch relationship[66,67] for conventional coarse-grained polycrystalline materials suggests that the hardness or yield strength of a material increases with a decreasing grain size according to the equation

$$\sigma = \sigma_0 + Kd^{-1/2}$$

where d is the grain diameter, σ is the 0.2 pct yield stress, σ_0 is the lattice friction stress to move individual dislocations, and K is a constant. Accordingly, nanocrystalline materials are expected to show much higher yield strengths. But, the slope K for a hardness or yield strength *vs* $d^{-1/2}$ plot is much lower in the nanometer range than is seen at more normal grain sizes. However, it should be realized that the above equation has certain limitations. First, the strength value cannot increase indefinitely to beyond the theoretical strength limit. Second, any relaxation processes taking place at the grain boundaries (due to the very fine grain size) could lead to a decrease in strength and, thus, an inverse $d^{-1/2}$ relationship below some critical grain size. Third, it should be realized that the Hall-Petch relationship was derived on the basis of strengthening due to dislocation pileups at physical obstacles. At extremely fine grain sizes, *e.g.*, in the nanometer regime, the individual grains cannot support more than one dislocation; and thus, the Hall-Petch relationship may not be valid. (The interested reader is referred to Reference 68 for a critical discussion of the influence of grain size on mechanical properties of conventional polycrystalline materials and the various dislocation models for explaining the Hall-Petch relation.) Thus, it is logical to expect that the mechanism of hardening/softening observed in nanocrystalline materials may be fundamentally different from that observed in coarser grained metals.

Some attempts have been made recently to rationalize the apparently conflicting results obtained on the hardness/yield strength of nanocrystalline materials as a function of grain size.

Since dislocation pileups are required for the Hall-Petch relation to be followed and because the pileups cannot form in materials with a grain size $d < l_c$, (where l_c is the dislocation spacing in the pileup[69]), Nieh and Wadsworth[70] suggested that when the grain size is below l_c, other weakening mechanisms, *e.g.*, viscous type flow, set in and lead to a decrease in hardness with decreasing grain size. This could explain the situation in nanocrystalline Cu (d = 8 to 16 nm and l_c = 19.3 nm) and Pd (d = 7 to 13 nm and l_c = 11.2 nm). The negative

Table II. Properties of Nanocrystalline Metals Compared with Their Crystalline and Glassy Counterparts[1,7]

Property	Material	Crystal	Glass	Nanocrystal
Thermal expansion (10^{-6}/K)	Cu	16	18	31
Specific heat at 295 K (J/g/K)	Pd	0.24	—	0.37
Density (g/cc)	Fe	7.9	7.5	6
Elastic moduli (GPa)				
Young's modulus	Pd	123	—	88
Shear modulus	Pd	43	—	32
Saturation magnetization at 4 K (emu/g)	Fe	222	215	130
Susceptibility (10^{-6} emu/Oe/g)	Sb	− 1	− 0.03	20
Fracture stress (GPa)	Fe-1.8 pct C	0.7	—	8
Superconducting T_c (K)	Al	1.2	—	3.2
Activation energy for diffusion (eV)	Ag in Cu	2.0	—	0.39*
	Cu in Cu	2.04	—	0.64
Debye temperature (K)	Fe	467	—	3

*Between 303 and 343 K and 0.63 eV between 353 and 373 K.

slope in Ni-P specimens has been explained[70] on the basis of the precipitation hardening due to the formation of Ni_3P on thermal annealing. However, this reasoning does not explain all of the results obtained to date.[71]

As mentioned earlier, the grain boundary component of the metal increases substantially as the grain size decreases. However, it has been recently pointed out that triple junctions form an important component of the microstructure at very small grain sizes.[72] In fact, the triple junction volume fraction displays a greater grain size dependence than the grain boundary volume fraction. For example, the triple junction volume fraction increases by three orders of magnitude in the range of 100 to 2 nm, while in the same range, the grain boundary volume fraction increases by little over one order of magnitude. Thus, the negative Hall-Petch slope at very small grain sizes in Cu, Pd, and Ni-P samples has been explained on the basis of increased triple junction volume fraction at these grain size levels,[73] since it has been earlier reported[74] that increased triple junction volume fractions lead to softening and enhanced bulk ductility in polycrystalline materials.

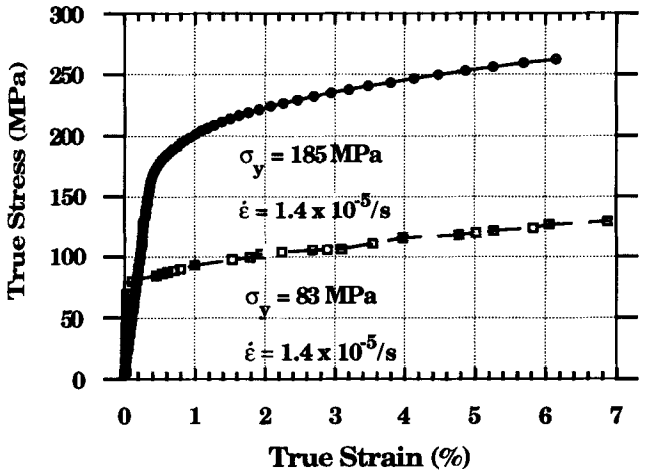

Fig. 7 — Stress-strain curves for nanocrystalline (25 nm) (●) and coarse-grained (50 μm) (□) copper sample.[61]

Very high hardness[43] and tensile strength values[45] compared to normal polycrystalline material have been reported for nanocrystalline alloys produced by MA. It has been suggested that these enhanced mechanical properties are due to the fact that deformation in these materials cannot occur by dislocation gliding.[43] Cryomilling (MA at liquid nitrogen temperature) leads to a matrix of fine-grained (50 to 300 nm) aluminum with dispersed 2- to 10-nm-diameter aluminum oxynitride particles.[75] This microstructure proved to be very resistant to coarsening, even at temperatures approaching the melting point of the material.

The fine grain sizes and the high rates of diffusivity observed in the nanocrystalline materials suggest that considerable creep deformation can occur even at room temperature, since according to the Coble creep model, the creep rate is proportional to D_b/d^3, where D_b is the grain boundary diffusivity and d is the average grain diameter. This is indeed observed in nanocrystalline TiO_2 and CaF_2 ceramic materials.[11] However, constant-stress creep measurements on nanocrystalline Cu and Pd samples[51,61] show that the observed creep rates at room temperature are at least three orders of magnitude smaller than predicted on the basis of the Coble creep model. These observations require further investigation.

B. *Layered Nanocrystals*

Unlike the situation in equiaxed nanocrystalline materials, the Hall-Petch-type relationship appears to be obeyed in layered nanocrystalline materials when the microhardness is plotted as a function of the layer thickness. This observation has been verified in vacuum-deposited Al-2 to 15.3 wt pct Fe alloys with the Fe layer spacing varying between 0.2 and 2.9 nm[8] and also in Cu-15 to 60 wt pct Fe alloys.[76] The layer thickness here is defined as the sum of the individual layer thicknesses of the constituent metals.

Hardwick[30] has recently reviewed methods for the determination of thin-film mechanical properties with emphasis on their strengths and limitations. The strength properties of multilayer deposits (1-D nanocrystals) have been calculated both theoretically[77] and experimentally.[78–81] Koehler[77] theoretically evaluated the effect

of alternate thin layers of pure metals (or other materials) with differing elastic constants on the ability of a Frank-Read dislocation source to operate. He predicted that dislocations will require a large externally applied force to cause them to move from the material of lower elastic constant into the material with the higher elastic constant. When the lamellar thickness is small enough, the Frank-Read source may not operate at all, in either layer, leading to a situation in which single dislocations are the mechanism by which plastic deformation occurs. This suggests that the thin nanocrystalline layered structure should exhibit resistance to plastic deformation and brittle fracture well beyond levels exhibited by monolithic homogeneous metals.[79] It can be predicted that the Frank-Read source will not be able to operate because of the restricting effect of the thickness (t) of the lamellar nanostructure when

$$t \leq 32\ \pi \mathbf{b}/R$$

where **b** is the Burger's vector of the Frank-Read source dislocations and R is the ratio of the difference in elastic constants divided by the sum of the elastic constants.[77-79,82] This implies that when the layer thickness is less than the dimension of the dislocation source, the interface between the two layers restricts dislocation generation because of the extreme bowing that the pinned dislocation line segments would have to assume to continue to operate. For an Fe-Al nanostructure, this equation predicts that Koehler strengthening will occur when the layer thickness of aluminum is less than about 47 nm.[82]

These theoretical predictions have been experimentally confirmed. Lehoczky[78,79] found that the tensile yield strength of Al-Cu increased inversely as the first power of the layer thickness down to a value of 70 nm. Below 70 nm, the yield strength was 620 MPa and the ultimate tensile strength 700 MPa, about 4 times greater than predicted from rule-of-mixtures. For Al-Ag laminates, where the difference in elastic moduli is much less than in Al-Cu, the critical layer thickness for Koehler strengthening was 230 nm and the strength increment was not significant.

The work by Lehoczky[78,79] was a clear demonstration of the validity of the predictions made by Koehler.[77] Dramatic increases in microhardness and yield strength have also been reported for electron beam vapor-deposited Al-Fe multilayer deposits,[8] epitaxially evaporated layers of Ni/Cu films,[81] and electrodeposited 90 pct Ni-10 pct Cu layered structures for a Cu layer thickness below 400 nm.[80] At 10-nm thicknesses, strengths of about 1300 MPa were obtained, more than a factor of 2 above MONEL* 400 (66.5 pct Ni-33.5 pct Cu) and 3 times above 98 pct Ni-2 pct Cu. In all cases, elongations in the range of 2 to 4 pct were noted. This work was subsequently extended down into the smaller thickness regime by Menezes and Anderson,[83] who demonstrated that a maximum tensile strength occurred at a nominal Cu layer thickness of 2 nm (18-nm-thick Ni layer).

*MONEL is a trademark of Inco Alloys International, Inc., Huntington, WV.

Tribological (wear) studies indicated that composition-modulated Ni-Cu layer coatings of 10- and 100-nm layer thickness offered increased resistance to both lubricated and unlubricated sliding wear against steel than pure metal (Ni or Cu) coatings, and the coating with the small layer spacing showed the least wear, particularly at low loads. This improved wear behavior was attributed to both mechanical strengthening (the Koehler effect), *i.e.*, resistance to wear deformation, and to a suitable boundary film formation in the presence of paraffin oil.[84,85,86]

C. *Supermodulus Effect*

The elastic moduli of the layered structures have been found to be strongly dependent on the thickness of the layers. At a critical thickness of about 2 nm, the modulus sharply increased by a factor of 4 (Figure 8), and this has been referred to as the supermodulus effect.[87,88,89] This effect, however, is observed only in some cases (*e.g.*, Cu-Ni, Cu-Pd, Au-Ni, Ag-Pd) and only in multilayered films that were highly [111] textured.[87] Table III summarizes the available data on the supermodulus effect in multilayer deposits.[90-97]

Theoretical models to explain the supermodulus effect fall into two main groups.[87] The first, a purely electronic interpretation, considers the interaction of the Fermi surface with the artificial Brillouin zone boundary created by the compositional modulation in the multilayer.[98] An elastic strain would tend to drag the zone and the Fermi surface out of contact, resulting in destabilization that would manifest itself in a stiffer crystal. This model predicts critical periodicities that should lead to

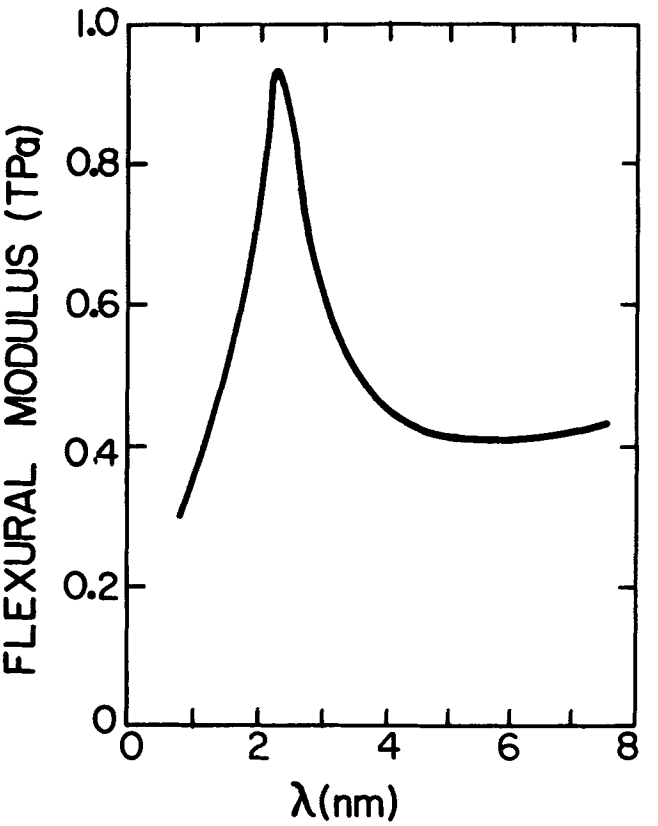

Fig. 8—Variation of the flexural modulus with the wavelength of modulation in as-deposited Cu-Ni foils of constant composition (about 50 at. pct Cu) and [111] texture.[93]

Table III. Supermodulus Effect in Layered Nanocrystals

Lattice Structures	Component Couple	Mutual Solubility	Pct Lattice Mismatch	Supermodulus Effect	References
Fcc-fcc	Au-Ni	miscible	13.5	yes	90
	Cu-Pd	miscible	7.5	yes	90
	Ag-Pd	miscible	4.9	yes	91
	Cu-Ni	miscible	2.5	yes	92, 93
	Cu-Au	miscible	12.7	no	91
	Pt-Ni			no	94
Bcc-fcc	Nb-Cu	immiscible	8.9	no	95
	Mo-Ni	immiscible	10.8	no	96
Hcp-fcc	Ti-Ni	immiscible	19.0	no	97

anomalously enhanced stiffness and wavelengths of critical contact close to 2 nm. A serious shortcoming of this model is that it predicts both enhancements and reductions in the moduli in the same system as the entire composition modulation wavelength range is scanned; such a result is not observed experimentally. Further, the thermal stability of the modulated structures has been explained on the basis of energy changes associated with the Fermi surface-Brillouin zone interactions. However, the easy homogenization of the modulated films even on low-temperature annealing strongly suggests that any electronic energy changes associated with the modulation are small and unlikely to affect the elastic moduli.

The existence of large coherency strains that can be generated in well-matched layers is the basis of the other major theory to explain the supermodulus effect. Since the coherency strains can be as large as a few percent, they can result in atomic displacements out of the Hookean region of the interatomic potential, leading to modulus enhancements. Since these changes are due to an odd (third) order effect, they can cause either increases or decreases in the elastic constants, depending on whether the layer is under compression or under tension.[88,99] Further, this model is consistent with the homogenization upon annealing. However, this approach cannot explain the origin of the sharpness of the maximum and also why the modulus increase is not observed below about 2 nm. One possibility is that the falloff in stiffness might result from glass formation by interdiffusion, the so-called solid-state amorphization process,[100] and it has been reported[96] that Mo-Ni films show evidence of a crystalline-to-amorphous transition as a function of modulation wavelength. However, the supermodulus effect is not observed in Cu-Au modulated films, where coherency strains are large, even though it is observed in Cu-Ni films having smaller coherency strains due to closeness of the lattice parameters.

Thus, both theories are deficient in explaining all of the observations, and more refined theories and further experimental data are needed to provide an unambiguous explanation of the supermodulus effect. For example, one can investigate whether the supermodulus effect will be observed in other like-lattice types (*e.g.*, bcc-bcc and hcp-hcp) and whether the reduction occurs in other dissimilar lattice types (*e.g.*, fcc-hcp and bcc-hcp). Additional experiments with metals having different extents of coherency can also establish the relative roles of coherency strains and electronic effects as the causes for the supermodulus effect. Recently, it has been suggested[101] that the supermodulus effect in multilayered thin films is due (at least in part) to nonlinear elastic effects caused by the large elastic biaxial strains generated in *all* of the layers by the surface stresses of *incoherent* interfaces. This could explain the modulation wavelength dependence as well as the approximate magnitude of the supermodulus effect.

Since the microhardness and yield strength of the multilayer deposits increase by a factor of 4 to 5 as the layer thickness decreases,[8,102–104] this implies a parallel with the supermodulus effect for metals with dissimilar crystal lattices (*e.g.*, fcc-bcc), while in other cases, the increase in strength with a decrease in layer thickness may be explained by invoking the Hall-Petch relationship.

In all of the above cases, it should be remembered that the mechanical properties of the samples will be influenced by the impurity concentration (both during formation and subsequent processing of the nanocrystals), grain size or lamellar thickness variations, type and nature of interfaces, porosity, and presence of cracks.

VI. CONCLUDING REMARKS

Nanocrystalline metals of the equiaxed, layered, and filamentary types appear to offer signficant physical and mechanical property advantages over conventional polycrystalline metals. In the equiaxed crystallite area, expanded alloying possibilities, high ductilities, and improved mechanical performance appear to offer the major advantages for structural applications. It has been demonstrated that below a critical grain size, macroscopically brittle materials, such as ceramics and intermetallics, become macroscopically ductile. This enhanced ductility can improve the processability, after which the material can be converted to a conventional-scale structure.

The microstructure and mechanical properties of the equiaxed crystallites are only now beginning to be investigated in detail. The nature and morphology of grain boundaries and other microstructural features (triple junctions, intragrain defects, *etc.*) are yet to be fully characterized and compared with coarse-grained material. It is still being debated whether the Hall-Petch relationship is obeyed at these fine grain sizes.

The majority of the investigations on equiaxed nanostructures to date have been concerned with materials

having a grain size of 5 to 10 nm. Conventional fine-grained polycrystalline materials have grain sizes of about 1000 nm or larger. Hence, materials with grain sizes of about 100 nm and also those in the 1- to 2-nm range should be evaluated to determine the full range of possible properties as a function of grain size.

Again, for layered metal nanostructures, we are at an early stage of exploration. The prospect of tailoring both strength (Koehler effect) and elastic modulus (supermodulus effect) by varying the layer thickness is an exciting possibility. The effect of changing the layer behavior by alloying, dispersion strengthening, and by combining metals and nonmetals should allow even higher combinations of strength and stiffness to be obtained. The increased resistance to wear of the layered nanostructures also offers some interesting applications, as does development of novel textures. And in an overall tailoring concept, corrosion behavior also can be controlled by the layer thickness. Filamentary metal nanostructures offer perhaps the greatest potential but are also at the earliest stage of development, with only a few scattered articles in the literature.

It will be interesting to compare more completely the behavior of nanocrystalline, conventional crystalline metals and glassy alloys as potential engineering materials. Several comparisons have been made between crystalline and glassy alloys. However, a majority of the nanocrystalline phases have been observed in pure metals, while conventional engineering alloys and glassy alloys are multicomponent systems. As such, a meaningful comparison is difficult because of lack of sufficient data on equivalent systems.

ACKNOWLEDGMENTS

The authors wish to acknowledge valuable discussions with Professor H. Gleiter of the University of Saarlandes, Saarbrücken, Federal Republic of Germany, Dr. R.W. Siegel of the Argonne National Laboratory, Argonne, IL, Dr. D. Tench of the Rockwell International Science Center, Thousand Oaks, CA, and G.W. Nieman of Northwestern University, Evanston, IL. They also wish to thank Mrs. Susan Goetz for formulating and typing this manuscript.

REFERENCES

1. H. Gleiter: *Prog. Mater. Sci.*, 1989, vol. 33, pp. 223-315.
2. B.H. Kear, L.E. Cross, J.E. Keem, R.W. Siegel, F. Spaepen, K.C. Taylor, E.L. Thomas, and K-N. Tu: NMAB Report 454, National Academy Press, Washington, DC, 1989.
3. R.W. Siegel: *MRS Bull.*, 1990, vol. 15 (10), pp. 60-67.
4. R. Birringer: *Mater. Sci. Eng. A*, 1989, vol. A117, pp. 33-43.
5. F.H. Froes and C. Suryanarayana: JOM (*J. Miner. Met. Mater. Soc.*), 1989, vol. 41 (6), pp. 12-17.
6. R.P. Andres, R.S. Averback, W.L. Brown, L.E. Brus, W.A. Goddard III, A. Kaldor, S.G. Louie, M. Moscovits, P.S. Peercy, S.J. Riley, R.W. Siegel, F. Spaepen, and Y. Wang: *J. Mater. Res.*, 1989, vol. 4, pp. 704-36.
7. C. Suryanarayana and F.H. Froes: in *Physical Chemistry of Powder Metals Production and Processing*, W. Murray Small, ed., TMS, Warrendale, PA, 1989, pp. 279-96.
8. R.L. Bickerdike, D. Clark, J.N. Easterbrook, G. Hughes, W.N. Mair, P.G. Partridge, and H.C. Ranson: *Int. J. Rapid Solidification*, 1984-85, vol. 1, pp. 305-25.
9. B.M. Gallois, R. Mathur, S. Lee, and J.Y. Yoo: in *Multicomponent Ultrafine Microstructures*, L.E. McCandlish, D.E. Polk, R.W. Siegel, and B.H. Kear, eds., MRS, Pittsburgh, PA, 1989, vol. 132, pp. 49-60.
10. R.W. Siegel, S. Ramasamy, H. Hahn, Li Zongquan, Lu Ting, and R. Gronsky: *J. Mater. Res.*, 1988, vol. 3, pp. 1367-72.
11. J. Karch, R. Birringer, and H. Gleiter: *Nature*, 1987, vol. 330, pp. 556-58.
12. M.J. Mayo, R.W. Siegel, A. Narayanasamy, and W.D. Nix: *J. Mater. Res.*, 1990, vol. 5, pp. 1073-82.
13. T. Mütschele and R. Kirchheim: *Scripta Metall.*, 1987, vol. 21, pp. 1101-04.
14. Y. Waseda: *The Structure of Non-Crystalline Materials*, McGraw-Hill, New York, NY, 1980.
15. C. Suryanarayana and F.H. Froes: in *Materials with Ultrafine Microstructures, Proc. Acta Metall. Conf.*, Atlantic City, NJ, Oct. 1990, in press.
16. E.L. Joyce, Jr. and T.R. Jervis: *Scripta Metall.*, 1988, vol. 22, pp. 1313-16.
17. K. Kimoto, Y. Kamiya, M. Nonoyama, and R. Uyeda: *Jpn. J. Appl. Phys.*, 1963, vol. 2, pp. 702-13.
18. C.G. Granquist and R.A. Buhrman: *J. Appl. Phys.*, 1976, vol. 47, pp. 2200-19.
19. D.S. Lashmore and M.P. Dariel: in *Encyclopedia of Materials Science and Engineering*, R.W. Cahn, ed., Pergamon Press, Oxford, United Kingdom, 1988, suppl. vol. 1, pp. 136-40.
20. *New Materials by Mechanical Alloying Techniques*, E. Arzt and L. Schultz, eds., Deutsche Gesellschaft für Metallkunde, Oberursel, Federal Republic of Germany, 1989.
21. B.A. Joyce: *Rep. Prog. Phys.*, 1985, vol. 48, pp. 1637-97.
22. T.R. Anantharaman and C. Suryanarayana: *Rapidly Solidified Metals: A Technological Overview*, TransTech Publications, Aedermannsdorf, Switzerland, 1987.
23. Y. Yoshizawa, S. Oguma, and K.J. Yamauchi: *J. Appl. Phys.*, 1988, vol. 64, pp. 6044-46.
24. T.R. Jervis and L.R. Newkirk: *J. Mater. Res.*, 1986, vol. 1, pp. 420-24.
25. K. Lu, W.D. Wei, and J.T. Wang: *Scripta Metall. Mater.*, 1990, vol. 24, pp. 2319-23.
26. K. Lu, J.T. Wang, and W.D. Wei: *Scripta Metall. Mater.*, 1991, vol. 25, pp. 619-23.
27. J.A. Eastman: in *Multicomponent Ultrafine Microstructures*, L.E. McCandlish, D.E. Polk, R.W. Siegel, and B.H. Kear, eds., MRS, Pittsburgh, PA, 1989, vol. 132, pp. 27-34.
28. U. Cohen, F.B. Koch, and R. Sard: *J. Electrochem. Soc.*, 1983, vol. 130, pp. 1987-95.
29. D.S. Lashmore and M.P. Dariel: *J. Electrochem. Soc.*, 1988, vol. 135, pp. 1218-21.
30. D.A. Hardwick: *Thin Solid Films*, 1987, vol. 154, pp. 109-24.
31. R. Sundaresan and F.H. Froes: JOM (*J. Min. Met. Mater. Soc.*), 1987, vol. 39 (8), pp. 22-27.
32. C.C. Koch: *Ann. Rev. Mater. Sci.*, 1989, vol. 19, pp. 121-43.
33. E. Hellstern, H.J. Fecht, Z. Fu, and W.L. Johnson: *J. Appl. Phys.*, 1989, vol. 65, pp. 305-10.
34. J.S.C. Jang and C.C. Koch: *Scripta Metall. Mater.*, 1990, vol. 24, pp. 1599-1604.
35. H.J. Fecht, G. Han, Z. Fu, and W.L. Johnson: *J. Appl. Phys.*, 1990, vol. 67, pp. 1744-48.
36. H.J. Fecht, E. Hellstern, Z. Fu, and W.L. Johnson: *Metall. Trans. A*, 1990, vol. 21A, pp. 2333-37.
37. E. Hellstern, H.J. Fecht, C. Garland, and W.L. Johnson: in *Multicomponent Ultrafine Microstructures*, L.E. McCandlish, D.E. Polk, R.W. Siegel, and B.H. Kear, eds., MRS, Pittsburgh, PA, 1989, vol. 132, pp. 137-42.
38. E. Hellstern, H.J. Fecht, Z. Fu, and W.L. Johnson: *J. Mater. Res.*, 1989, vol. 4, pp. 1292-95.
39. J.S.C. Jang and C.C. Koch: *J. Mater. Res.*, 1990, vol. 5, pp. 498-510.
40. T. Christman and M. Jain: *Scripta Metall. Mater.*, 1991, vol. 25, pp. 767-72.
41. C.C. Koch and Y.S. Cho: in *Materials with Ultrafine Microstructures, Proc. Acta Metall. Conf.*, Atlantic City, NJ, Oct. 1990, in press.
42. P.H. Shingu, B. Huang, S.R. Nishitani, and S. Nasu: *Suppl. Trans. Jpn. Inst. Met.*, 1988, vol. 29, pp. 3-10.
43. W. Schlump and H. Grewe: in *New Materials by Mechanical Alloying Techniques*, E. Arzt and L. Schultz, eds., Deutsche Gesellschaft für Metallkunde, Oberursel, Federal Republic of Germany, 1989, pp. 307-18.

44. C.C. Koch, J.S.C. Jang, and S.S. Gross: *J. Mater. Res.*, 1989, vol. 4, pp. 557-64.
45. P.H. Shingu, B. Huang, J. Kuyama, K.N. Ishihara, and S. Nasu: in *New Materials by Mechanical Alloying Techniques*, E. Arzt and L. Schultz, eds., Deutsche Gesellschaft für Metallkunde, Oberursel, Federal Republic of Germany, 1989, pp. 319-26.
46. C. Suryanarayana and F.H. Froes: *J. Mater. Res.*, 1990, vol. 5, pp. 1880-86.
47. G.W. Nieman, J.R. Weertman, and R.W. Siegel: in *Clusters and Cluster-Assembled Materials*, R.S. Averback, J. Bernholc, and D.L. Nelson, eds., MRS, Pittsburgh, PA, 1991, vol. 206, pp. 493-98.
48. G.J. Thomas, R.W. Siegel, and J.A. Eastman: *Scripta Metall. Mater.*, 1990, vol. 24, pp. 201-06.
49. H.-E. Schaefer, R. Würschum, R. Birringer, and H. Gleiter: *Phys. Rev. B*, 1988, vol. B38, pp. 9545-54.
50. G.W. Nieman, J.R. Weertman, and R.W. Siegel: *Scripta Metall.*, 1989, vol. 23, pp. 2013-18.
51. G.W. Nieman, J.R. Weertman, and R.W. Siegel: *Scripta Metall. Mater.*, 1990, vol. 24, pp. 145-50.
52. H. Hahn, J.L. Logas, and R.S. Averback: *J. Mater. Res.*, 1990, vol. 5, pp. 609-14.
53. H.-E. Schaefer, R. Würschum, R. Birringer, and H. Gleiter: *J. Less-Common Met.*, 1988, vol. 140, pp. 161-69.
54. J. Horvath, O.R. Birringer, and H. Gleiter: *Solid State Commun.*, 1987, vol. 62, pp. 319-22.
55. R. Birringer, H. Hahn, H. Höfler, J. Karch, and H. Gleiter: *Defect Diffusion Data*, 1988, vol. 59, pp. 17-32.
56. S. Schumacher, R. Birringer, R. Strauss, and H. Gleiter: *Acta Metall.*, 1989, vol. 37, pp. 2485-88.
57. R. Kirchhiem, T. Mütschele, W. Kieninger, H. Gleiter, R. Birringer, and T.D. Koble: *Mater. Sci. Eng.*, 1988, vol. 99, pp. 457-62.
58. R. Bohn, T. Haubold, R. Birringer, and H. Gleiter: *Scripta Metall. Mater.*, 1991, vol. 25, pp. 811-16.
59. D. Korn, A. Morsch, R. Birringer, W. Arnold, and H. Gleiter: *J. Phys. (Paris)*, 1988, vols. 49, colloq. 5, pp. 769-79.
60. M. Weller, J. Diehl, and H.-E. Schaefer: *Phil. Mag. A*, in press.
61. G.W. Nieman, J.R. Weertman, and R.W. Siegel: *J. Mater. Res.*, 1991, vol. 6, pp. 1012-27.
62. G.W. Nieman, J.R. Weertman, and R.W. Siegel: in *Clusters and Cluster-Assembled Materials*, R.S. Averback, J. Bernholc, and D.L. Nelson, eds., MRS, Pittsburgh, PA, 1991, vol. 206, pp. 581-86.
63. G.D. Hughes, S.D. Smith, C.S. Pande, H.R. Johnson, and R.W. Armstrong: *Scripta Metall.*, 1986, vol. 20, pp. 93-97.
64. H.J. Höfler and R.S. Averback: *Scripta Metall. Mater.*, 1990, vol. 24, pp. 2401-06.
65. A.H. Chokshi, A. Rosen, J. Karch, and H. Gleiter: *Scripta Metall.*, 1989, vol. 23, pp. 1679-84.
66. E.O. Hall: *Proc. Phys. Soc. (London)*, 1951, vol. B64, pp. 747-53.
67. N.J. Petch: *J. Iron Steel Inst.*, 1953, vol. 174, pp. 25-28.
68. A. Lasalmonie and J.L. Strudel: *J. Mater. Sci.*, 1986, vol. 21, pp. 1837-52.
69. V.G. Gryaznov, V.A. Solov'ev, and L.I. Trusov: *Scripta Metall. Mater.*, 1990, vol. 24, pp. 1529-34.
70. T.G. Nieh and J. Wadsworth: *Scripta Metall. Mater.*, 1991, vol. 25, pp. 955-58.
71. C. Suryanarayana, D. Mukhopadhyay, S.N. Patankar, and F.H. Froes: *J. Mater. Res.*, in press.
72. G. Palumbo, S.J. Thorpe, and K.T. Aust: *Scripta Metall. Mater.*, 1990, vol. 24, pp. 1347-50.
73. G. Palumbo, U. Erb, and K.T. Aust: *Scripta Metall. Mater.*, 1990, vol. 24, pp. 2347-50.
74. V.B. Rabukhin: *Phys. Met. Metall.*, 1986, vol. 61, p. 149.
75. M.J. Luton, C.S. Jayanth, M.M. Disko, S. Matras, and J. Vallone: in *Multicomponent Ultrafine Microstructures*, L.E. McCandlish, D.E. Polk, R.W. Siegel, and B.H. Kear, eds., MRS, Pittsburgh, PA, 1989, vol. 132, pp. 79-86.
76. L.S. Palatnik, A.I. Il'inskii, and N.P. Sapelkin: *Soviet Phys.-Solid State*, 17, vol. 8, pp. 2016-17.
77. J.S. Koehler: *Phys. Rev. B.*, 1970, vol. 2, pp. 547-51.
78. S.L. Lehoczky: *J. Appl. Phys.*, 1978, vol. 49, pp. 5479-85.
79. S.L. Lehoczky: *Phys. Rev. Lett.*, 1978, vol. 41, pp. 1814-18.
80. D. Tench and J. White: *Metall. Trans A*, 1984, vol. 15A, pp. 2039-40.
81. K. Yoshii, H. Takagi, M. Umeno, and H. Kawabe: *Metall. Trans. A*, 1984, vol. 15A, pp. 1273-80.
82. A. Kelly: *Phil. Trans. R. Soc. London*, 1987, vol. A322, pp. 409-23.
83. S. Menezes and D. Anderson: Electrochemical Society Meeting, Chicago, IL, 1988, Abstract 342.
84. A.W. Ruff and N.K. Myshkin: *J. Tibol.*, 1989, vol. 111, pp. 156-60.
85. A.W. Ruff, N.K. Myshkin, and Z.X. Wang: *Proc. Int. Conf. on Engineered Materials for Advanced Friction and Wear Applications*, ASM INTERNATIONAL, Metals Park, OH, 1988, pp. 41-46.
86. A.W. Ruff and Z.X. Wang: *Wear*, 1989, vol. 131, pp. 259-72.
87. R.C. Cammarata: *Scripta Metall.*, 1986, vol. 20, pp. 479-86.
88. T. Tsakalakos and A.F. Jankowski: *Ann. Rev. Mater. Sci.*, 1986, vol. 16, pp. 293-313.
89. T. Tsakalakos and A.F. Jankowski: in *Multicomponent Ultrafine Microstructures*, L.E. McCandlish, D.E. Polk, R.W. Siegel, and B.H. Kear, eds., MRS, Pittsburgh, PA, 1989, vol. 132, pp. 199-212.
90. W.M.C. Yang, T. Tsakalakos, and J.E. Hilliard: *J. Appl. Phys.*, 1977, vol. 48, pp. 876-79.
91. G.E. Henein and J.E. Hilliard: *J. Appl. Phys.*, 1983, vol. 54, pp. 728-33.
92. T. Tsakalakos and J.E. Hilliard: *J. Appl. Phys.*, 1983, vol. 54, pp. 734-37.
93. D. Baral, J.B. Ketterson, and J.E. Hilliard: *J. Appl. Phys.*, 1985, vol. 57, pp. 1076-83.
94. B.M. Clemens and G.L. Eesley: *Phys. Rev. Lett.*, 1988, vol. 61, pp. 2356-59.
95. A. Kueny, M. Grimsditch, K. Miyano, I. Banerjee, C.M. Falco, and I.K. Schuller: *Phys. Rev. Lett.*, 1982, vol. 48, pp. 166-70.
96. M.R. Khan, C.S.L. Chung, G.P. Flecher, M. Grimsditch, A. Kueny, C.M. Falco, and I.K. Schuller: *Phys. Rev. B.*, 1982, vol. 27, pp. 7186-93.
97. D. Tench: Rockwell International, Thousand Oaks, CA, private communication, May 1989.
98. P.C. Clapp: *Modulated Structure Materials*, NATO-ASI Series, Applied Sciences, T. Tsakalakos, ed., Martinus-Nijhoff, Dordrecht, The Netherlands, 1985, pp. 455-64.
99. A.F. Jankowski and T. Tsakalakos: *J. Phys. F, Metal Phys.*, 1985, vol. 15, pp. 1279-92.
100. W.L. Johnson: *Prog. Mater. Sci.*, 1986, vol. 30, pp. 81-134.
101. R.C. Cammarata and K. Sieradzki: *Phys. Rev. Lett.*, 1989, vol. 62, pp. 2005-08.
102. M.D. Merz and S.D. Dahlgren: *J. Appl. Phys.*, 1975, vol. 46, pp. 3235-37.
103. R.W. Springer and D.S. Catlett: *Thin Solid Films*, 1978, vol. 54, pp. 197-205.
104. R.F. Bunshah, R. Nimmagadda, H.J. Doerr, B.A. Movchan, N.I. Grechanuk, and E.V. Dabizha: *Thin Solid Films*, 1980, vol. 72, pp. 261-75.